scientific reports

Check for updates

OPEN

Design of an innovative aptasensor for the detection of chemotherapeutic drug Fludarabine phosphate

Shamsa Alanazi[1], Amina Rhouati[1], Amani Chrouda[2], Dana Cialla-May[3,4], Jürgen Popp[3,4], Saddam Muthana[1], Majed Dasouki[5] & Mohammed Zourob[1]✉

Monitoring the concentration of Fludarabine phosphate, a standard chemotherapeutic drug widely used in cancer treatment, is vital for ensuring the drug's safety and effectiveness, tailoring treatments to individual needs, and consequently improving overall patient outcomes. Regarding the limitations of conventional techniques in terms of complexity, large time measurements, and a high cost, there is an urgent need to develop simple, rapid, and cost-effective devices. In this paper, we report the design of an aptasensor for the specific and selective detection of Fludarabine. Systematic evolution of ligands by exponential enrichment (SELEX) protocol was performed to select a specific aptamer for Fludarabine. Eleven rounds were carried out, and nine sequences were selected. Based on the dissociation constant (Kd), Ful-3, exhibiting the highest affinity (18.86 nM), was chosen and integrated into a simple electrochemical aptasensing platform for Fludarabine detection. Electrochemical results demonstrated good performance of the selected aptamer in detecting Fludarabine within the analytical range of 1 to 150 pg/mL and with LOD and LOQ in the order of 0.11 pg/mL (0.31 fM) and 0.39 pg/mL (1.06 fM), respectively. The developed platform also showed good selectivity against different analogous molecules and high applicability in serum-spiked samples, with recovery percentages ranging from 96.81 to 99.04%. Considering the encouraging results, this research presents an excellent alternative in terms of simplicity, stability, ease of use, reduction of sample volume, and low cost.

Keywords Chemotherapeutic drug, Fludarabine phosphate, Aptamer, Anticancer, Biosensor

Many nucleoside analogues have been approved as therapeutic agents in different clinical applications. Among them, cytotoxic derivatives are widely employed as antineoplastic drugs mainly in hematologic malignancies and solid tumors[1]. First, the pyrimidine analogue Cytarabine has shown excellent results with leukemia patients. Then, other compounds have been discovered such as Vidarabine which was reported as unstable because of its insolubility and sensitivity to deactivation by adenosine deaminase[2]. It is noteworthy that the enzymatic pattern including, intracellular deaminating, phosphorylating, and dephosphorylating enzymes, influence directly the activation and deactivation of nucleoside analogs and thus their therapeutic effects. To overcome these limitations, further investigations have been carried out to discover new compounds from the nucleoside analogs family. For that, fluorine atom has been added to vidarabine, to inhibit deamination while the solubility was enhanced by adding a phosphate atom[3]. Clinical trials have demonstrated that the resulting compound called Fludarabine phosphate (9-β -D-arabynofuranosyl-2-fluoroadenine monophosphate) was more efficient and well tolerated by patients[4].

Fludarabine phosphate (Fludara®) is mainly used for the treatment of adult patients with B-cell chronic lymphocytic leukemia (CLL) and non-Hodgkin's lymphoma (NHL) in addition to Waldenström's macroglobulinemia (WM)[5]. After intravenous administration, the drug is dephosphorylated in plasma, and undergoes stepwise phosphorylation into the cell, yielding the active form Fludarabine-ATP[6]. This active

[1]Department of Chemistry, Alfaisal University, Al Zahrawi Street, Al Maather, Al Takhassusi Rd, Riyadh 11355, Saudi Arabia. [2]Department of Chemistry, College of Science Al Zulfi, Majmaah University, Zulfi, Saudi Arabia. [3]Institute of Physical Chemistry and Abbe Center of Photonics, Friedrich Schiller University, Jena, Germany. [4]Leibniz Institute of Photonic Technology, Member of Leibniz Health Technologies, Member of the Leibniz Centre for Photonics in Infection Research (LPI), Albert-Einstein-Straße 9, 07745 Jena, Germany. [5]King Faisal Specialist Hospital and Research Center, (KFSHRC), Takhussessi street, Riyadh, Saudi Arabia. ✉email: mzourob@alfaisal.edu

metabolite can suppress DNA and RNA synthesis by inhibiting DNA polymerase, ribonucleotide reductase, and DNA primase, thus leading to apoptosis[7]. As a pronounced immunosuppressive drug, Fludarabine phosphate has several side effects such as myelosuppression, neurotoxicity and neuropathy fevers[8]. To avoid these outcomes, the recommended intravenous dosage regimen for CLL was fixed as 25 to 30 mg/m^2 during five days, until achieving a plasma concentration of 3 µmol/L at the end of each infusion[9]. However, the pharmacokinetic and pharmacodynamic profile of the drug varies from patient to patient, thus requiring a personalized approach to the dosage regimen[7,10]. Therefore, sensitive analytical methods are highly required to enable Fludarabine phosphate monitoring in biological samples. In general, this analysis is performed by chromatographic techniques, such as HPLC (high performance liquid chromatography)[4,11] and LC-MS/MS (liquid chromatography tandem mass spectrometry)[12]. Despite their accuracy and sensitivity, these methods are based on sophisticated and expensive equipment requiring qualified staff and specialized laboratories as well as long pre-treatment steps. In addition, large volumes of reagents and blood samples are needed for the detection procedure. In this context, biosensors have emerged as an excellent alternative to the traditional analytical techniques in different fields, in particular biomedical applications[13–15]. Satana et al. studied the in situ electrochemical valuation of Fludarabine phosphate based on its interaction with double stranded DNA with a limit of detection of 0.05 pM[16]. However, to the best of our knowledge, no affinity biosensor has been reported for Fludara determination. For that reason, we describe in this report the first electrochemical aptasensor to monitor Fludara concentration in blood.

Biosensors are simple analytical devices based on the specific binding between a biological component and its target. The biological response is then converted to a physical measurable signal related to the amount of the analyte in the sample[17]. Different bioreceptors can be used for recognition, including enzymes, antibodies, peptides, DNA probes and aptamers. Since their discovery in 1990, aptamers have attracted much attention because of their advantageous features[18]. Aptamers are short and single stranded oligonucleotides, characterized by their high ability to attach their analytes with high affinity and specificity. They are selected in vitro, by a simple selection process called SELEX (Systematic evolution of ligands by exponential enrichment), without the animal immunization required for antibodies generation[19]. In addition, they are more stable, cost-effective and reproducible compared to antibodies which suffer from batch-to-batch variations[20,21]. For these reasons, we investigate in this work the applicability of aptamers in antineoplastic analysis with a focus on Fludarabine-phosphate drug. To achieve that, SELEX process was carried out by performing iterative rounds of selection and amplification. Sequences generated from the eighth round underwent a negative selection to eliminate non-specific candidates. After 11 rounds of SELEX, ten sequences (Flu-1 to Flu-10) were cloned, aligned and sequenced. Then, affinity studies were realized to determine each aptamer dissociation constant *(Kd)*. Finally, the aptamer exhibiting the best affinity against Fludarabine phosphate was integrated in a label-free electrochemical biosensing platform. The selectivity of the proposed aptasensor was studied with different potential interferents including chemotherapeutic drugs and antibiotics. The analytical performance of the Fludara aptasensor was also investigated in real serum samples. We believe that the developed aptasensor provides an affordable assay for rapid detection and quantification of Fludarabine phosphate that could be used by frontline healthcare workers and hopefully will improve patient follow up during chemotherapy. Moreover, the selected aptamer can be used in other analytical assays using electrochemical or optical detection.

Experimental section

DNA library design and preparation of the Fludarabine-conjugated beads

A DNA library of 1015 sequences was synthesized by Metabion, Germany. Each sequence comprises, 40 random nucleotides flanked by fixed regions of 16 nucleotides at both 5′ and 3′ ends for primers binding (5'-TCCCTA CGGCGCTAAC-N40-GCCACCGTGC-TACAAC-3'). Fluorescein-labelled forward primer designed was used for (polymerase Chain reaction) PCR amplification to enable the DNA quantification during SELEX rounds. In parallel, the targeted analyte (Fludarabine phosphate) was conjugated with NHS-activated sepharose beads according to the manufacturer's protocol. First, the beads were washed several times with 1 M (Hydrochloric Acid) HCl solution and incubated with 100 µL (5 mg/mL) of Fludarabine solution on a rotator at 4 °C overnight. Then, after the mixture centrifugation for 5 min at 300 rpm, the supernatant was eliminated, and the beads were washed alternately with 2 mL of 0.1 M (tris Sodium Chloride) tris NaCl and acetate NaCl three times each. Finally, the beads coupled to the drug were stored in 0.1 M tris buffer at 4 °C.

In vitro selection of Fludara aptamers

Prior to the selection process, 100 µL of Fludarabine-conjugated sepharose beads were washed five times with 400 µL of binding buffer. In parallel, the DNA library was pretreated by heating at 90 °C for 5 min and cooling at 4 °C for 10 min. After that, the DNA library was added to the prepared beads and left to react under rotation for 2 h at room temperature. The beads were then washed with binding buffer until no fluorescence was detectable in the washes. The DNA oligonucleotides bound to Fludarabine-coupled beads were eluted with 300 µL of elution buffer. The elution buffer consisted of 7 M urea dissolved in binding buffer and heated for 10 min at 90 °C. The operation was repeated until no fluorescence was detected in the last elution. Finally, the eluted DNA was collected and concentrated with a 3 kDa cutoff membrane filter. The resulting DNA was amplified by PCR where the mix was composed of 2 units of Taq Plus polymerase, 1x taq buffer, 2 mM $MgCl_2$, 200 mM dNTP, 0.2 mM of forward and reverse primers. The PCR mixture was thermocycled at 94 °C for 7 min, followed by 25 cycles of 94 °C for 45 s, 47 °C for 45 s, 72 °C for 45 s, and a final extension step of 10 min at 72 °C. The amplified dsDNA was revealed by running 2% agarose gel electrophoresis in Tris base, acetic acid and EDTA buffer(TAE buffer) using ethidium bromide as a fluorescent marker under 110 V for 30 min. The double stranded DNA (dsDNA) PCR product was precipitated by adding 0.1 volume of 3 M sodium acetate and 3 volumes of cold ethanol and incubated at 80 °C for one hour, then centrifuged for 30 min at 4 °C. The precipitate was washed with 75% cold ethanol and re-suspended in 50:50 water and a mixture of loading dye in formamide and heated

to 90 °C for 5 min. The DNA strands labelled with fluorescein were separated by 10% denaturing PAGE at 300 V for 2.30 h. The fluorescent ssDNA band was cut from the gel and treated with freeze-thaw cycles in Tris, EDTA buffer (TE) buffer followed by incubation at 37 °C overnight. Finally, the eluted single strand DNA (ssDNA) was concentrated by ultrafiltration using a 3 kDa cutoff membrane filter and used for the next round of selection.

For the counter selection (CS) cycle, the DNA pool from the 8th round was utilized. The ssDNA was incubated with blank sepharose beads and the flow-through and unbound DNA from the blank beads were collected and concentrated. The collected DNA was then subjected to the same heating and cooling treatments as described earlier, and then it was incubated with Fludarabine-conjugated beads for the next round of SELEX.

Cloning, sequencing and alignment of the selected aptamers specific to Fludarabine phosphate

After the different rounds of SELEX, the resulting DNA was cloned to identify the ssDNA sequences. For that, a fresh PCR was performed under the following conditions: 95 °C for 5 min, 15 cycles of 95 °C and 54 °C for 30 s each, and 72 °C for 45 s, followed by a 10-minute extension at 72 °C. The DNA was then ligated with a cloning vector, which was added into competent *E. coli* cells using heat shock. Afterwards, the cells were added to a prewarmed Optimal broth with Catabolite repression (SOC) medium and incubated at 37 °C for one hour. Next, Luria broth (LB) agar plates were prepared with 50 µg/mL ampicillin and 40 mg/mL X-Gal. Then, the SOC cell suspension was spread on the LB agar plates with different volumes and incubated overnight at 37 °C. The cells were then observed, where the white cells were selected. Afterwards, a PCR amplification was performed on the white cells with M13 primers, and the PCR tubes were collected, loaded onto a 2% agarose gel to identify the base pair length. Finally, PCR products were sequenced and aligned by using PRALINE multiple sequence alignment toolbox (http://ibivu.cs.vu.nl/programs/pralinewww/).

Determination of the dissociation constants *(kd)*

After the SELEX process, the obtained sequences were subjected to binding affinity studies for determining their dissociation constants. To achieve that, Fluorescein-labelled aptamers were synthesized after eliminating the primers-binding sites and the *Kds* of the selected aptamers were determined by performing fluorescence binding assays. Each fluorescein-labelled sequence was pretreated before binding by heating at 90 °C for 10 min, followed by cooling at 4 °C for 10 min and then 25 °C for 5 min. Afterwards, various concentrations of the labelled aptamers (from 0 to 400 nM) were incubated with Fludarabine-conjugated beads under rotation for 1 h at room temperature. After washing with binding buffer, the bound DNA was eluted from the beads by adding the elution buffer at 90 °C for 10 min and centrifuging at 13,000 rpm for 1 min. Then, the eluted DNA from each sample was determined by fluorescence measurement at 515 nm using a nanodrop spectrophotometer. For each aptamer sequence, a saturation curve was plotted, and the *Kd* values were calculated by nonlinear regression fitting of the curve.

Electrochemical aptasensing of Fludarabine phosphate

Aiming to investigate their applicability in Fludarabine detection, the selected aptamers were used to develop an electrochemical aptasensing platform. For that, the aptamer sequence with the highest affinity, lowest values were modified with a thiol group to enable its covalent binding to a gold screen printed gold electrode (SPGE). In brief, 10 µL of the aptamer solution (1µM) was incubated on the gold working electrode overnight at 4 °C. After that, the electrodes were washed with 0.1 M Phosphate buffered saline (PBS) buffer. Based on the literature, we select to block active sites with 6-Mercaptohexanol (MCH) for 1 h[22]. For detection, the functionalized electrodes were incubated with 10 µL of different concentrations of fludarabine for 30 min, separately. Finally, the electrochemical response was recorded by square wave voltammetry (SWV) in 5 mM Ferricyanide $[Fe(CN)_6]^{3-/4-}$ solution prepared in 0.1 M PBS buffer.

To evaluate the specificity of the developed aptasensor to Fludara drug, the aptamer-functionalized gold electrode was incubated with 10 µL of different drugs at a fixed concentration of 100 pg/mL. Then, the electrochemical response of the aptasensor was recorded for each interfering drug by SWV. Two chemotherapeutic drugs (5-fluorouracil and Docetaxel) and three antibiotics (Amoxicillin, Penicillin and Doxycycline) were selected to perform the cross-reactivity studies.

For clinical validation, the aptasensor analytical performance was tested on human serum samples (purchased from Sigma-Aldrich-UK). To achieve that, the real samples were spiked with different concentrations of Fludara drug. Then, 10 µL of each sample was incubated on the modified gold surface and left for 30 min at room temperature. Following this, the electrodes were washed with PBS and then subjected to SWV measurements, as previously described.

Results and discussion

ssDNA selection and characterization of aptamers against Fludarabine phosphate

The binding of Fludara drug to the beads in SELEX is a crucial step that enables the separation of the bound and unbound DNA. Fludara was immobilized on NHS-activated Sepharose beads through its terminal amine groups. The NH_2 groups on the drug molecules were activated and then used to react with the terminal carboxyl groups on the beads through amide bond formation. After the covalent binding of Fludara molecules to the sepharose beads, 0.1 M of Tris was used to block the remaining unreacted amine groups on the beads. This step would minimize the non-specific electrostatic attraction of the DNA to sepharose beads. The prepared Fludara-conjugated sepharose beads were used for all the aptamer selection cycles. Each cycle consisted of two main steps: selection and amplification. For selection, the beads were incubated with the DNA library composed of 10^{15} random 40 nucleotide sequences followed by partitioning the bound and unbound DNA via binding buffer

washing. Then, the ssDNA candidates specifically bound to the Fludara-conjugated sepharose beads were eluted, PCR amplified and purified to obtain a new enriched DNA pool to start the subsequent SELEX cycle.

The DNA recovery after each cycle was monitored by measuring the fluorescence of the eluted DNA. A gradual increase in the recovered DNA was observed after each cycle. Eight rounds of positive selection were performed, after which a counter selection, consisting of incubating the DNA collected from the eighth round with negative unconjugated sepharose beads, was carried out. Negative selection is a crucial step to avoid the selection of aptamers exhibiting an affinity for the immobilization support. It has been demonstrated that the elimination of these non-specific candidates improves the affinity of the generated aptamers ten times[22]. Fig. 1 shows the fluorescence intensities obtained from the DNA measurements of aptamers eluted from each cycle.

As it can be seen from the histogram, the fluorescence intensity increased with successive SELEX cycles. After the counter selection, a significant decrease in the fluorescence intensity was noted at rounds 9 and 10, indicating the removal of the DNA that was non-specifically bound to the beads. Then, a dramatic increase in the fluorescence intensity was observed at rounds 10 and 11, implying the enrichment of the DNA pool with the specific sequences to Fludara. Therefore, the selection process was stopped after 11 rounds, and the recovered DNA was cloned into *E.coli* competent cells. The selected colonies were then picked up for amplification and sequencing. Finally, the identified sequences were grouped using the multiple sequence alignment software PRALINE (Supporting information).

Binding affinity studies of the selected aptamers towards Fludara

A total of ten sequences was generated from the aptamer's selection process. These sequences underwent a binding affinity study, to identify the most specific aptamers to our targeted analyte; Fludarabine phosphate drug. To enable the DNA quantification, the selected sequences were labeled with fluorescein. The study was carried out by incubating a fixed number of Fludarabine-conjugated beads with increasing concentrations (0 to 400 nM) of each fluorescently-labelled sequence, individually. Then, the unbound sequences were eliminated by washing and the bound sequences were eluted, and their fluorescence intensities were quantified at 515 nm. Afterwards, the binding curves were plotted for each aptamer sequence as the fluorescence intensity versus the DNA concentration. The dissociation constants (*Kd*s) of the various aptamer-target complexes were calculated by non-linear regression analysis of the binding curves. The aptamers sequences and dissociation constants are listed in Table 1.

The obtained *Kd* values range from 18.86 to 373.7 nM showing the success of the aptamer selection process towards Fludara with high affinity. As it can be seen from the table, Flu-3 exhibited the highest affinity with a *Kd* as low as 18.86 nM. Therefore, it was selected to pursue the following experiments.

Electrochemical biosensing of Fludara drug using the selected aptamers

Design of the apatasensor for Fludara detection

Flu-3 was employed in the fabrication of the electrochemical aptasensor for Fludarabine detection. The integration of the selected aptamer into an electrochemical platform was achieved through the covalent linking of SH groups labelling the ssDNA with the gold surface of the SPGE. This immobilization strategy was chosen for different reasons. First, it is a simple technique that doesn't require many steps or reagents. More importantly, the spontaneous adsorption of sulfur groups onto metal surfaces generates uniform layers of well oriented bioreceptors. In parallel, the inert properties of gold and its ability to form well-defined crystal structures

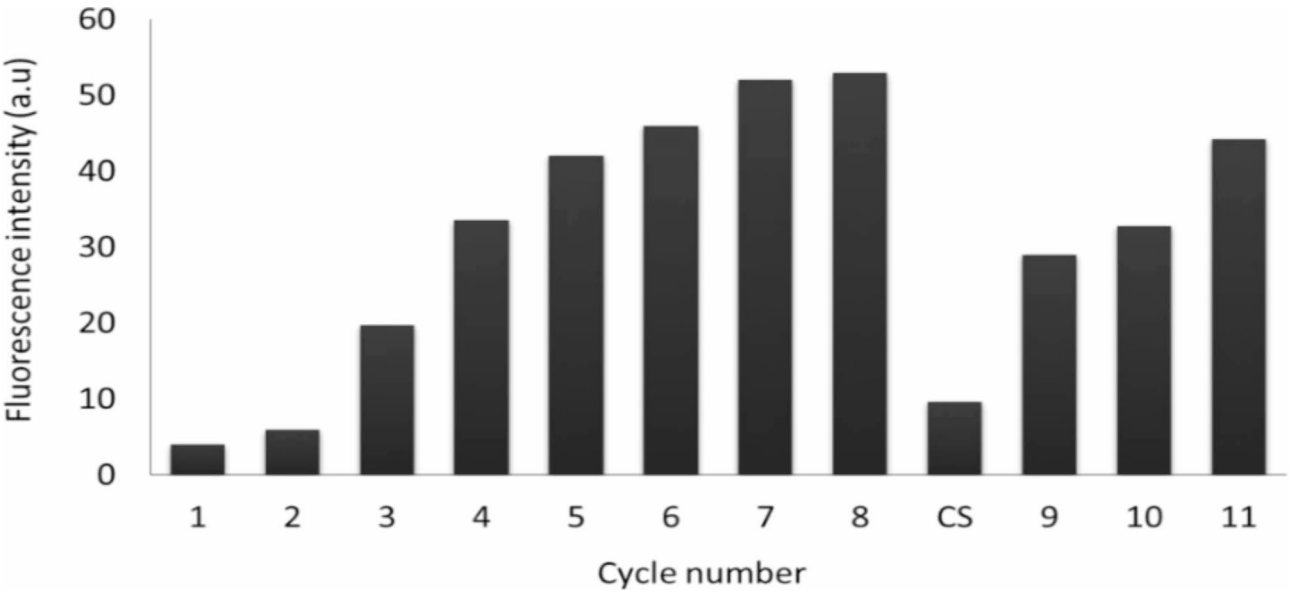

Fig. 1. Fluorescence intensity of the recovered amount of DNA measured after each round of SELEX.

Aptamer number	Sequence	Kd (nM)
F1	CCA CAC ACA TGT ACT GCG TCC GAA CTG TGT CCA CGT CCT CC	173.0
F2	CAC ACT CGT CAC TGA GGT TTG TGT CCA GTC TCA CTC GGA TT	739.0
F3	CCC AGG GTC CCA TCA GAT ATC GCA TTA CAT CAA TCA CCC GT	18.86
F4	CTA CAT TAG CCA AAA TAT CAG AAG ATA AGT AGG TAC GGT CG	39.05
F5	AGC TAT CCC GCA CCA ATC CAA CGT GAC CAG TGA GTT GAG G	266.4
F6	ACA GGT ACG TGC AGC CCC TGT GTT GTA CGG CCC ATC TGC A	20.43
F7	ACA GGT ACG TGC AGC CCC TGT GTT GTA CGG CCC ATC TGC A	Unstable
F8	CTA GGA CAA TGC CCG GGT GCG TTG TCG AAA CTC GAT AAT GA	386.3
F9	CAA CAG CAG AGG AAG GTA CGT TGC GAT GTG AAC CGT AGT GT	291.9

Table 1. Dissociation constants (K_d) calculated for the ten Fludara selected aptamers.

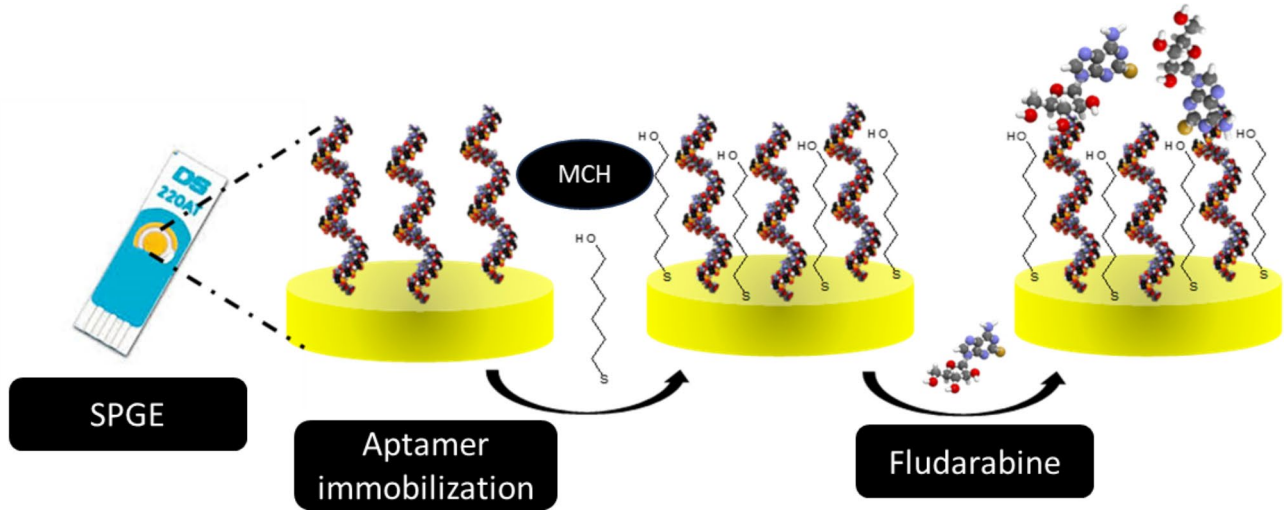

Fig. 2. Aptasensor design for Fludara drug detection.

influence strongly the generation of self-assembled monolayers leading to high density and excellent degree of regularity[23]. The surface modification process is illustrated on Fig. 2.

To confirm the successful linking of our aptamer onto the gold surface, electrochemical characterization was proceeded. For that, cyclic voltammetry measurements were conducted in redox solution (5mM ferri/ferrocyanide solution prepared in PBS buffer pH 7.4) within a potential range of (-0.6 to 0.6 V) and a scan rate of 100 mV/s. Figure 3A displays the cyclic voltammograms recorded on the bare gold surface (a), the aptamer functionalized surface (b) and the SPGE after MCH blocking step (c). As it can be seen from curve a and b, the chemisorption of thiols to gold resulted in a remarkable drop in the oxydo/reduction peaks. This decrease is certainly due to the formation of the aptamers monolayer which is based on three mains steps; diffusion-controlled physisorption and chemisorption of the thiolated-DNA, followed by the crystallization process[24]. Then, after the aptamer immobilization, MCH was used to displace the non-specific adsorption of DNA via nitrogen atoms thus enhancing the accessibility of aptamer molecules for Fludarabine. The corresponding cyclic voltammogram shows a decrease in the peak currents due to the repulsion between negatively charged DNA backbones and the negative dipole of the MCH alcohol terminus[25,26].

To improve the investigation of surface modification through various steps, electrochemical impedance spectroscopy was conducted under consistent conditions as shown in Fig. 3B. Initially, a very small semicircular domain with R_{CT}= 1.34 KΩι was recorded, indicating high surface conductivity. Following the biosensor modification with the aptamer, the R_{CT} value increased to 1.89 KΩι, and further increased to 4.67 KΩι after the addition of the blocking agent. This increase in electron transfer resistance confirms the successful immobilization of both the aptamer and MCH on the gold surface. The results obtained demonstrate good concordance between the electrochemical techniques used. To better control the surface morphology during the different modification steps, the subsequent section will elucidate TO surface analysis using SEM techniques.

Electrocatalytic study of the aptamer-modified surface

To better quantify the amount of aptamer covering the electrode surface, we calculated the surface area before and after modification with aptamer/SAM. To achieve this objective, we recorded the cyclic voltammetry (CV) voltammograms of the bare gold electrode and the gold electrode modified with aptamer and MCH, in response to varying scan rates using a redox probe. The obtained voltammograms are illustrated in Fig. 4A.

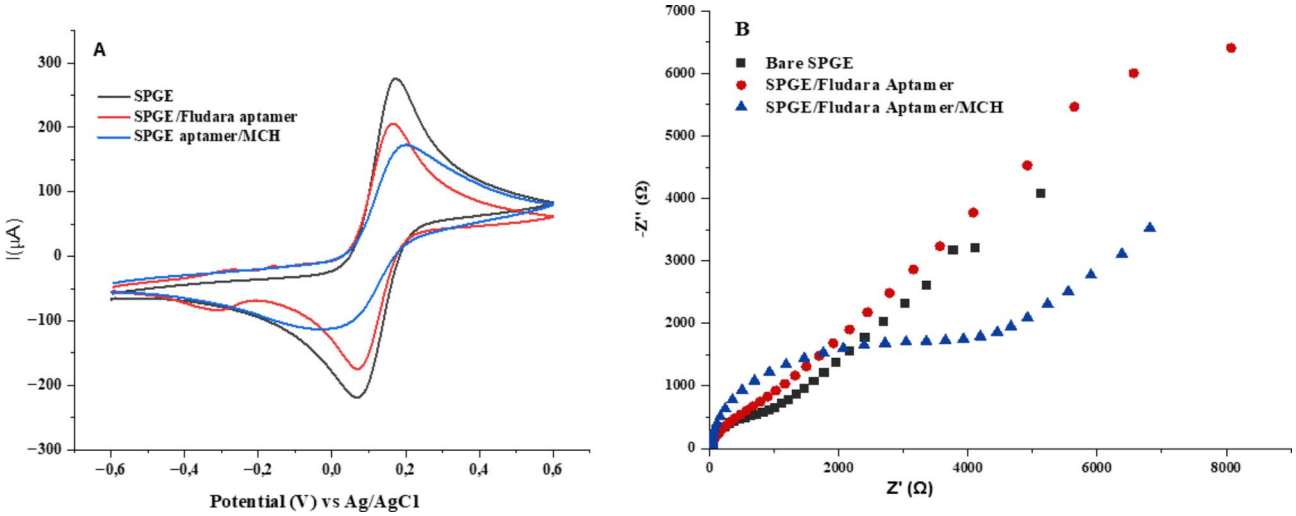

Fig. 3. (**A**) Cyclic voltammetry, (**B**) electrochemical impedance spectroscopy of bare gold electrode, Flu-3 aptamer modified electrode and after blocking with MCH. The CV and EIS measurements were recorded in the presence of $Fe(CN_6)^{3-/4-}$ as the redox probe, within a potential range of (-0.6 to 0.6 V) and a scan rate of 100 mV/s for CV and frequency range between 100 kHz and 0.1 Hz for EIS.

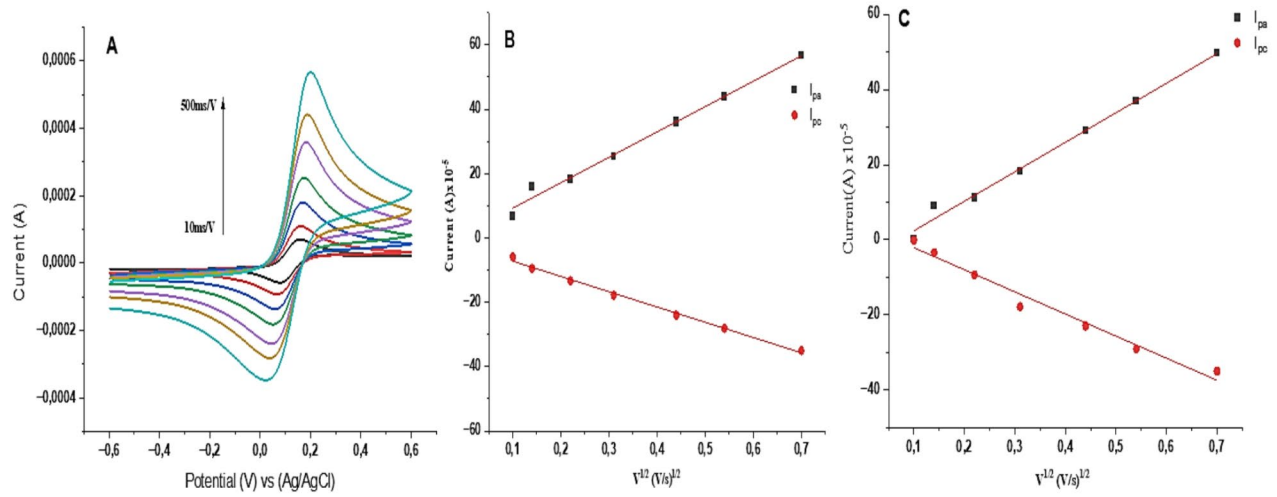

Fig. 4. (**A**) Cyclic voltammograms recorded at different scan rates (10, 20, 50, 100, 200, 300, 500 mV/s) in an equimolecular solution of 5 mM ferro/ferricyanide ($[Fe(CN)6]^{4-/3-}$), Plots of the peak current (Ip) versus the square root of the potential scan rate($v^{1/2}$) (**B**) on bare SPGE and (**C**) Flu-3- aptamer/ SPGE.

To enhance visualization of the CV variations, the oxidation and reduction currents versus the square root of the scan rate for the bare gold electrode and the modified electrode were plotted in Fig. 4B and C, respectively.

In both representations, a linear relationship between the oxidation and reduction peak current (ip) versus in visualized, revealing a diffusion-controlled oxidation process, permitting therefore the estimation of the diffusion coefficient of ferricyanide cation on bare gold (Fig. 4B). The D was found in the order of 24.62×10^{-6} $cm^2.s^{-1}$. By applying the Randles–Sevcik equation (Eq. (1), noted below), we have determined the surface area after modification (Table 2).

$$I_{pa} = \left(2{,}65 \times 10^5\right) n^{\frac{3}{2}} A D_0^{\frac{1}{2}} v^{1/2} C_0 \quad (1)$$

Where $I_{p.a.}$ refers to the anodic peak current, n is the number of electrons transferred, A is the dynamic surface area of electrode (cm^2), D_0 is the diffusion coefficient ($cm^2.s^{-1}$), v is the scan rate ($V.S^{-1}$), and C_0 is the concentration of $K_3Fe(CN)_6$ ($mol.cm^{-3}$).

The results obtained in Table 2 demonstrate a decrease in the geometric surface about only 7.7% compared the bare gold. Such variation reveals the effectiveness of the immobilization of biological layer (Flu-3 aptamer) on the surface of SPGE.

	Surface (Cm^2)	RSD (%)
Bare electrode (SPGE)	$S_{geo}=12\times10^{-2}$	4.3
Flu-3aptamer/SPGE	$S_{active}=11.2\times10^{-2}$	5.6

Table 2. Electroactive surface area after the modification of the SPGE with Flu-3, calculated from the CV scans performed in 5 mM $[Fe(CN)_6]^{4-/3-}$ equimolecular redox probe in PBS buffer pH (0.1 M, 7.4).

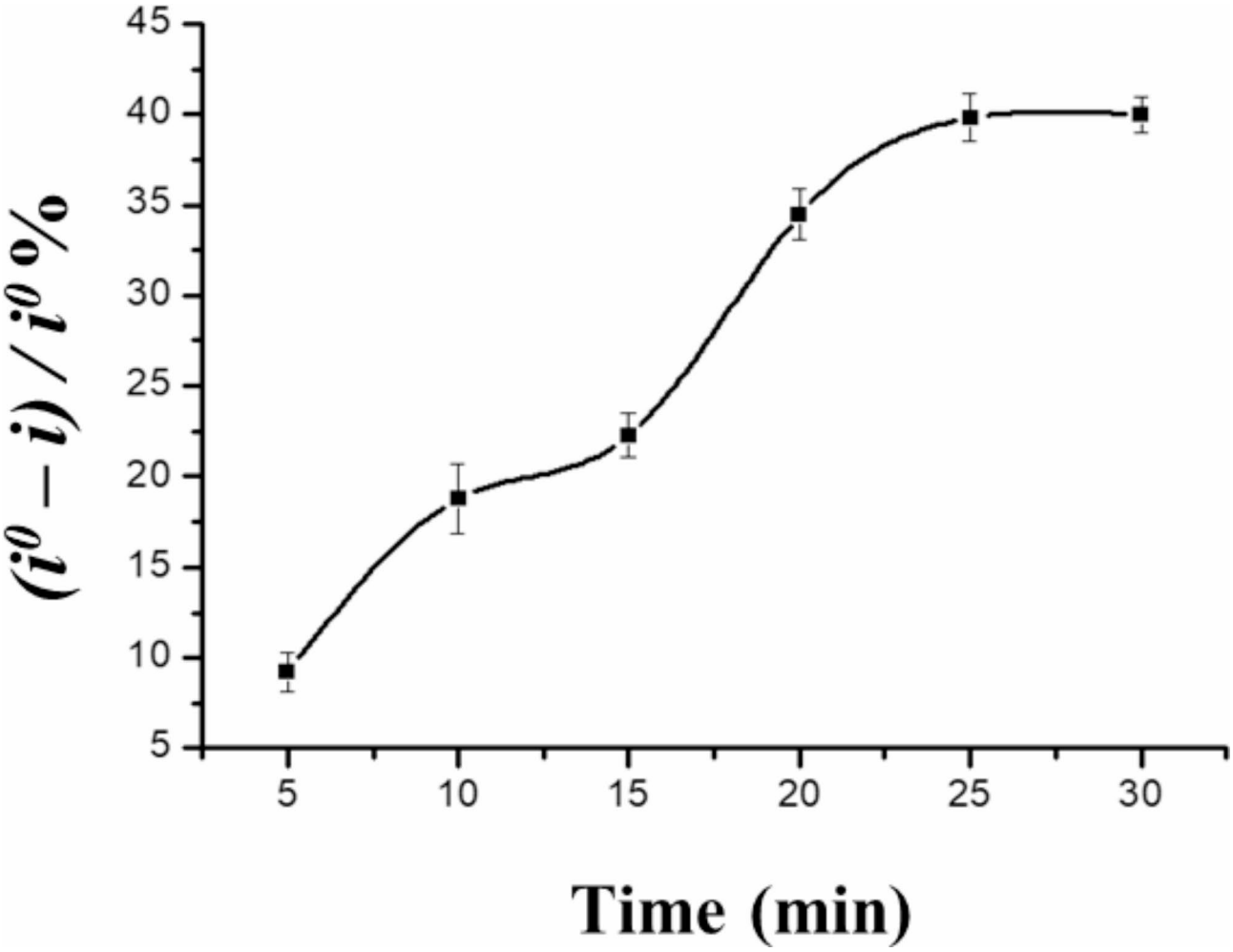

Fig. 5. Optimization of time incubation of aptamer incubation on the electrode surface.

Electrochemical detection of Fludarabine

The principle of the proposed aptasensor is based on monitoring the electrochemical behavior resulting from the specific binding between the aptamer and its target, Fludarabine phosphate. To enhance the analytical performance of the sensor, several parameters must be controlled and optimized, including the aptamer concentration, the aptamer immobilization time, and the analyte incubation time. Based on our previous investigations, we selected an aptamer concentration of 1 µM and an overnight incubation time for immobilization[27].

In parallel, to investigate the most appropriate time of Fludarabine incubation on the modified surface, the normalized variation of the output signal ($(i^0 - i) / i^0$%) is followed versus different incubation time ranging from 5 to 30 min, where i is the peak current obtained after incubating the aptasensor with Fludara (100 pg/mL) and i^0 is the peak current of the control. The obtained results are illustrated on Fig. 5.

The normalized current variation shows an increase versus time incubation from 5 to 25 min, until reaching a stability between 25 and 30 min. The results indicate that the appropriate time for a maximal binding and recognition between the aptamer and the molecule is in the order of 25 min.

Once the sensor performances are well optimized, the surface was incubated with increasing concentrations of Fludarabine, prepared in binding buffer, in the range of 1 to 150 pg/mL. The electrochemical measurements were carried out by SWV in the redox solution of 5mM ferri/ferrocyanide prepared in PBS buffer pH 7.4 in the potential range of (-0.2 to 0.5 V), frequency 25 Hz, interval time 0.04 s, step potential − 5 mV, scan rate 125 mV/s

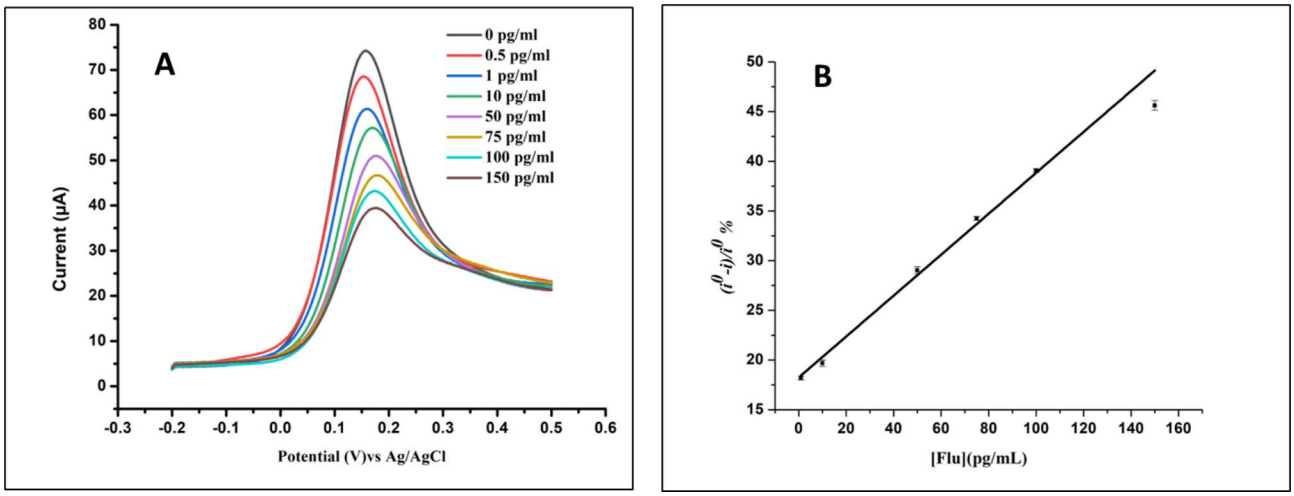

Fig. 6. (**A**) SWV voltammograms of the aptamer-functionalized electrode incubated with increasing concentrations of Fludarabine phosphate (0.5 to 150 pg/mL), (**B**) Calibration curve of Fludara: Plot of the aptasensor response $((i^0-i/i^0)\ \%)$ versus Fludara concentration (pg/mL). SWV was performed in 5mM ferri/ferrocyanide solution prepared in PBS buffer pH 7.4, potential range of (-0.2 to 0.5 V).

Technique	Linear range	LOD (pM)	Ref
HPLC	0.0125–10 nmol	25	[11]
HPLC	0.035–0.35 mg/ml	/	[28]
LC-MS/MS	0.25-10 µM	0.25×10^6	[12]
Isocratic LC	50-20000 pM	50	[29]
Fluorescence assay	2 pM-2 nM	2	[30]
dsDNA/GCE	1.6–14.8 µM	28×10^4	[31]
NH_2-MWCNTs/GCE	2.9×10^{-8} to 9.68×10^{-8} M	290	[32]
Flu-3- aptamer/ SPGE	2.81–422.7 fM	0.31×10^{-3}	This work

Table 3. Comparative table for the detection of Fludarabine phosphate using different methods.

and amplitude 20 mV. In parallel, a control experiment was realized by incubating the aptasensors with 10 µL of binding buffer (0 pg/mL of Fludarabine). Figure 6A shows the obtained SWV voltammograms after incubation of the gold electrode with the different concentrations of Fludarabine (1 to 150 pg/mL). From the figure, we observe that the peak current decreases by increasing the Fludarabine phosphate concentration. This decrease is mainly due to the formation of the complex aptamer-Fludarabine phosphate with high affinity and specificity. Therefore, this binding hampers the electron transfer to the gold surface resulting in decreasing current peaks. The electrochemical response of our aptasensor towards Fludara was subsequently determined based on the obtained peak currents. This response was then used to plot the calibration curve shown in Fig. 6B. As it can be observed from the figure, a good linearity was obtained for Fludara detection within the range of concentrations; 1 to 150 pg/mL.

The linear regression in the range of 1–150 pg/mL was as follows: $((i^0-i)/i^0\%)=18.25+0.20$ Fludara concentration (pg/mL) with R^2 equal to 0.99. The limit of detection limit as well as the limit of quantification were calculated as LOD = 3.3σ / S, and LOQ = 10σ / S respectively, where σ is the standard deviation of the blank and S is the slope. LOD and LOQ were found in the order of 0.11 pg/mL (0.31 fM) and 0.39 pg/mL (1.06 fM) respectively.

As mentioned in the introduction, electrochemical detection of Fludarabine using sensors is rarely reported in the literature. To highlight the analytical performance of the prepared sensor, particularly in term the limit of detection, we present a comparative analysis in Table 3. This table includes data from conventional techniques as well as sensors developed in silico for Fludarabine detection.

.

Table 3 illustrates that the present work, characterized by simplicity in preparation, rapidity, and low cost, demonstrates excellent performance with a very low limit of detection compared to conventional techniques and even to other designed electrochemical sensors.

Investigation of the analytical performance of the elaborated sensor

Reproducibility and repeatability Given that reproducibility is fundamental to the successful design, implementation, and adoption of sensors in healthcare, this parameter was investigated by following the electro-

chemical response of triplicate aptasensors prepared under the same conditions. The results demonstrated good reproducibility with an RSD of 4.5%, indicating the robustness of the prepared aptamers. Similarly, sensor stability over time is essential for ensuring reliable performance, reducing costs, meeting regulatory standards, and maintaining user trust. Therefore, stability was examined by recording the SWV measurements after 1, 7, and 15 days. The measurements demonstrated stability with deviations of 2%, 4%, and 8%, respectively. These results suggest the potential for repetitive sensor use, underscoring the stability of the aptamer designed using the SELEX method. Additionally, the repeatability of the proposed aptasensor was evaluated by recording five successive current signals, yielding an RSD of 1.99%.

Selectivity measurements Aiming to validate the clinical applicability of the selected aptamers as well as the fabricated aptasensor for Fludara monitoring, it was necessary to realize a cross-reactivity study. To achieve that, the Flu-3 functionalized SPGEs were incubated with different drugs including chemotherapeutics and antibiotics, separately. The analytical procedure was performed in the same experimental conditions and according to the protocol previously described for Fludara detection. In Fig. 7, a histogram comparing the aptasensor response towards Fludara with that of the potential interfering drugs: 5-fluorouracil, docetaxel, amoxicillin, penicillin and doxycycline.

From the histogram, we note that all the incubation of the non-specific drugs (100 pg/mL) with the functionalized gold surface didn't induce a peak decrease in the SWV measurements. Therefore, the corresponding responses based on the calculated ($(i^0-i)/i^0\%$) were all in negative order. Therefore, these findings confirm the excellent selectivity of our aptasensor to Fludarabine detection.

Real sample investigation In parallel, to demonstrate that the designed aptamer-based strategy could be applied in blood patients' samples without matrix effects, the aptasensor was tested with serum samples diluted (1: 100 in buffer solution). The Flu-3 modified SPGE were incubated with serum samples spiked with different concentrations of Fludarabine phosphate within the analytical range. Then, square wave voltammograms were recorded by using the same experimental conditions described above.

Finally, the recovery percentage was calculated by comparing the analytical response of the aptasensor in binding buffer with that in serum samples. Table 4 presents the added concentrations to each serum sample, the calculated concentrations, and the recovery percentages. The results showed excellent recovery percentages ranging from 96, indicating that the developed Fudara aptasensor can be successfully applied in biological fluids without interferences or matrix effects.

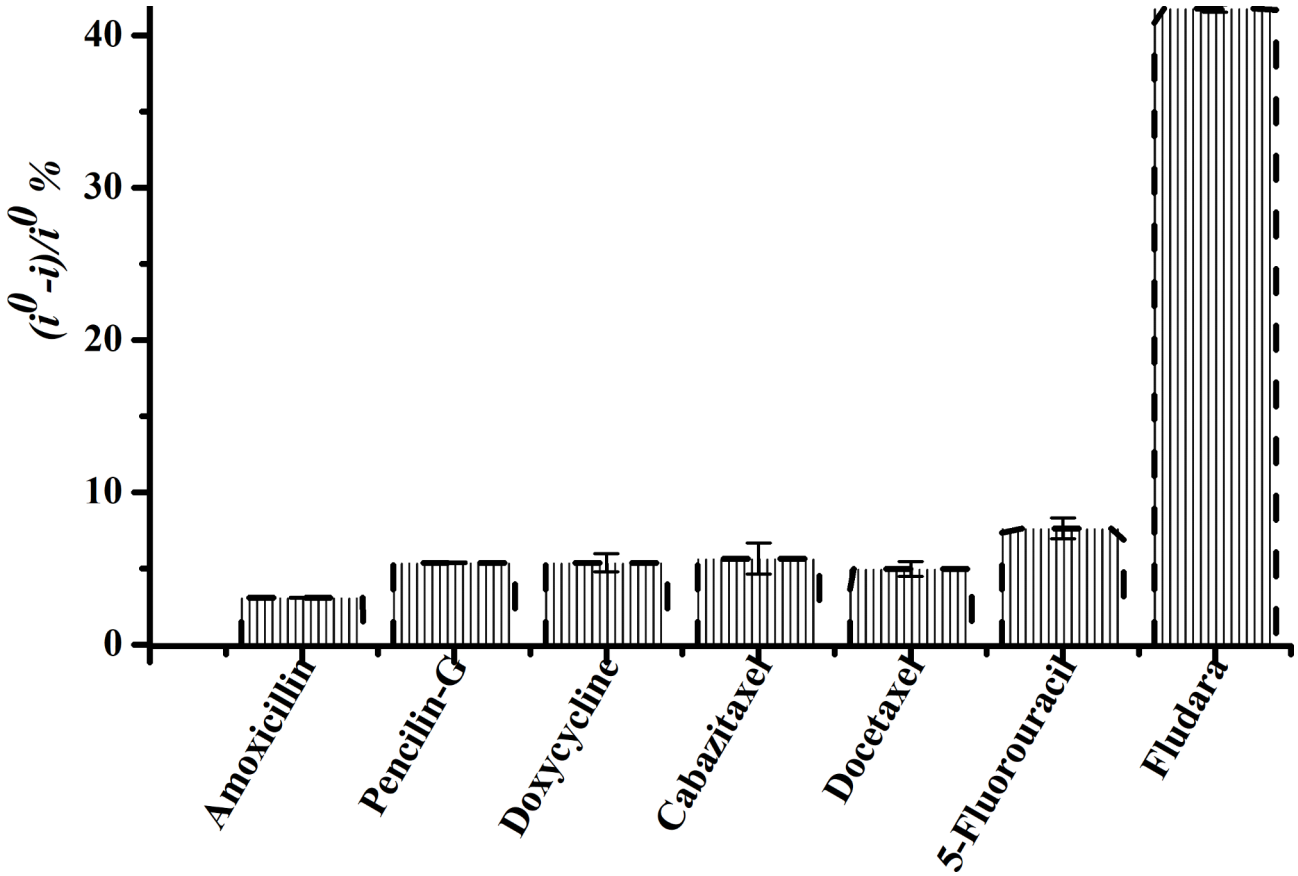

Fig. 7. Cross-reactivity study of the electrochemical Fludara aptasensor.

Added concentration (pg/mL)	Found concentration (pg/mL)	Recovery percentage (%)	*R*.S.D (%)
50	48.02	96.04	0.72
100	99.04	99.04	0.86
150	149.61	99.74	0.29

Table 4. Applicability of the proposed aptasensor for Fludara detection in serum spiked samples.

Conclusion

In summary, we selected the first aptamer for anticancer drugs monitoring by targeting the nucleoside analog Fludarabine phosphate commonly used in hematologic malignancies. The generated aptamer Flu-3 has shown a very good specificity and affinity for Fludara with the low *Kd* of 18.86 nM. As a first application of Flu-3 aptamer, we designed a simple label-free electrochemical biosensor to detect Fludarabine phosphate. The thiolated aptamer of 41 sequences was immobilized on a screen-printed gold electrode and the formation of the complex aptamer-Fludara was studied by SWV. Based on electrochemical analysis, Fludarabine phosphate can be detected within a wide linear range (1 to 150 pg/mL) with a high sensitivity which allows a LOD of 0.31 fM. Experiments on real serum samples demonstrated the potential clinical applicability of the aptasensor. Such an approach provides thus an effective promise to monitor Fludara levels during chemotherapy. Moreover, the designed biosensor can be miniaturized for in situ use thus helping healthcare professionals for a better understanding of Fludara pharmacokinetics and personalized treatments. Consequently, antineoplastic side effects could be easily mitigated.

Data availability

The data that support the findings of this study are available from the corresponding author upon reasonable request.

Received: 15 March 2024; Accepted: 28 October 2024
Published online: 01 November 2024

References

1. Cividini, F. et al. The purine analog fludarabine acts as a cytosolic 5′-nucleotidase II inhibitor. *Biochem. Pharmacol.* **94**(2), 63–68 (2015).
2. Hood, M. A. & Finley, R. S. *Fludarabine: Rev. DICP* **25**(5), 518–524 (1991).
3. Grever, M. et al. *A comprehensive phase I and II clinical investigation of fludarabine phosphate*. in *Seminars in oncology* (1990).
4. Ficarra, R. et al. Determination of fludarabine in a pharmaceutical formulation by LC. *J. Pharm. Biomed. Anal.* **21**(5), 1077–1081 (1999).
5. Goodman, E. R. & Fiedor, P. S. *Fludarabine phosphate: a DNA synthesis inhibitor with potent immunosuppressive activity and*. *Am. Surg.* **62**(6). (1996).
6. Yin, W. et al. Pharmacokinetics, bioavailability and effects on electrocardiographic parameters of oral fludarabine phosphate. *Biopharm. Drug Dispos.* **31**(1), 72–81 (2010).
7. Lichtman, S. M. et al. The pharmacokinetics and pharmacodynamics of fludarabine phosphate in patients with renal impairment: a prospective dose adjustment study. *Cancer Invest.* **20**(7–8), 904–913 (2002).
8. Ding, X. et al. Ocular toxicity of fludarabine: a purine analog. *Expert Rev. Ophthalmol.* **3**(1), 97–109 (2008).
9. Gandhi, V. & Plunkett, W. Cellular and clinical pharmacology of fludarabine. *Clin. Pharmacokinet.* **41**, 93–103 (2002).
10. Rodionov, G. et al. *Individual features of the pharmacokinetics of fludarabin phosphate in the treatment of patients with chronic lymphocytic leukemia*. *Kachestvennaya Klin. Praktika = Good Clin. Pract.*, **2021**(2), 67–77.
11. Rodriguez, C. O. Jr et al. High-performance liquid chromatography method for the determination and quantitation of arabinosylguanine triphosphate and fludarabine triphosphate in human cells. *J. Chromatogr. B Biomed. Sci. Appl.* **745**(2), 421–430 (2000).
12. Huang, L. et al. Determination of intracellular fludarabine triphosphate in human peripheral blood mononuclear cells by LC–MS/MS. *J. Pharm. Biomed. Anal.* **86**, 198–203 (2013).
13. Vilariño, N. et al. Use of biosensors as alternatives to current regulatory methods for marine biotoxins. *Sensors* **9**(11), 9414–9443 (2009).
14. Alhadrami, H. A. Biosensors: classifications, medical applications, and future prospective. *Biotechnol. Appl. Chem.* **65**(3), 497–508 (2018).
15. Eissa, S., Almusharraf, A. Y. & Zourob, M. A comparison of the performance of voltammetric aptasensors for glycated haemoglobin on different carbon nanomaterials-modified screen printed electrodes. *Mater. Sci. Engineering: C* **101**, 423–430 (2019).
16. GÜRSAN, K. A. E. et al. Electrochemical DNA biosensors developed for the monitoring of biointeractions with drugs: a review. *Turk. J. Chem.* **47**(5), 864–887 (2023).
17. Park, M. Surface display technology for biosensor applications: a review. *Sensors*. **20**(10), 2775 (2020).
18. Tuerk, C. & Gold, L. Systematic evolution of ligands by exponential enrichment: RNA ligands to bacteriophage T4 DNA polymerase. *Science* **249**(4968), 505–510 (1990).
19. Eissa, S. et al. Electrochemical SELEX technique for the selection of DNA aptamers against the small molecule 11-deoxycortisol. *ACS Appl. Bio Mater.* **2**(6), 2624–2632 (2019).
20. Adachi, T. & Nakamura, Y. Aptamers: a review of their chemical properties and modifications for therapeutic application. *Molecules* **24**(23), 4229 (2019).
21. Arshavsky-Graham, S. et al. Aptamers vs. antibodies as capture probes in optical porous silicon biosensors. *Analyst* **145**(14), 4991–5003 (2020).
22. Zhuo, Z. et al. Recent advances in SELEX technology and aptamer applications in biomedicine. *Int. J. Mol. Sci.* **18**(10), 2142 (2017).
23. Luderer, F. & Walschus, U. *Immobilization of oligonucleotides for biochemical sensing by self-assembled monolayers: thiol-organic bonding on gold and silanization on silica surfaces*. *Immobilisation DNA Chips I* 37–56. (2005).
24. Oberhaus, F. V., Frense, D. & Beckmann, D. Immobilization techniques for aptamers on gold electrodes for the electrochemical detection of proteins: a review. *Biosensors* **10**(5), 45 (2020).

25. Levicky, R. et al. Using self-assembly to control the structure of DNA monolayers on gold: a neutron reflectivity study. *J. Am. Chem. Soc.* **120**(38), 9787–9792 (1998).
26. Herne, T. M. & Tarlov, M. J. Characterization of DNA probes immobilized on gold surfaces. *J. Am. Chem. Soc.* **119**(38), 8916–8920 (1997).
27. Shaukat, A. et al. *Cell-based SELEX Aptamer Selection for Electrochemical Detection of Fluoribacter bozemanae Bacteria*15. 100411 (X, 2023).
28. Puy, J. Y. et al. Determination and quantification of intracellular fludarabine triphosphate, cladribine triphosphate and clofarabine triphosphate by LC–MS/MS in human cancer cells. *J. Chromatogr. B* **1053**, 101–110 (2017).
29. Yamauchi, T. & Ueda, T. Simple and sensitive method for quantification of fludarabine triphosphate intracellular concentration in leukemic cells using isocratic liquid chromatography. *J. Chromatogr. B* **799**(1), 81–86 (2004).
30. Kemena, A. et al. A sensitive fluorescence assay for quantitation of fludarabine and metabolites in biological fluids. *Clin. Chim. Acta* **200**(2–3), 95–106 (1991).
31. Eda Satana, H. & Oliveira-Brett, A. M. Situ evaluation of Fludarabine-DNA Interaction using a DNA-Electrochemical Biosensor. *Int. J. Electrochem.* **2011**(1), 340239 (2011).
32. Dogan-Topal, B. et al. Electrochemical determination and in silico studies of fludarabine on NH2 functionalized multiwalled carbon nanotube modified glassy carbon electrode. *Electroanalysis* **32**(1), 37–49 (2020).

Acknowledgements

The Authors extend their appreciation to the King Salman Center for Disability Research for Funding this work under Research Group No. KSRG-2023-478.

Author contributions

S.A., A. R. S.M did most of the experimental parts, A.C. helped in some experiments and proof reading, D.C.-M. J.P. M. Z. supervised the work and secured the funding, M.D. initiated the idea and proof read the mansucript.

Declarations

Competing interests

The authors declare no competing interests.

Additional information

Supplementary Information The online version contains supplementary material available at https://doi.org/10.1038/s41598-024-78039-5.

Correspondence and requests for materials should be addressed to M.Z.

Reprints and permissions information is available at www.nature.com/reprints.

Publisher's note Springer Nature remains neutral with regard to jurisdictional claims in published maps and institutional affiliations.